Planetary and Space Science 76 (2013) 28–41

Contents lists available at SciVerse ScienceDirect

Planetary and Space Science

journal homepage: www.elsevier.com/locate/pss

Gas–solid carbonation as a possible source of carbonates in cold planetary environments

A. Garenne [b,*], G. Montes-Hernandez [a,**], P. Beck [b], B. Schmitt [b], O. Brissaud [b], A. Pommerol [c]

[a] CNRS and University Joseph Fourier, ISTerre/UMR 5275, OSUG/INSU, BP 53, 38041 Grenoble Cedex 9, France
[b] CNRS and University Joseph Fourier, IPAG, OSUG/INSU, BP 53, 38041 Grenoble Cedex 9, France
[c] Physikalisches Institut, Universität Bern, Sidlerstrasse 5, CH-3012 Bern, Switzerland

ARTICLE INFO

Article history:
Received 3 April 2012
Received in revised form
8 November 2012
Accepted 9 November 2012
Available online 1 December 2012

Keywords:
Carbonates
Gas–solid carbonation
Mars
Low temperature
Infrared microscopy
Ca and Mg hydroxides

ABSTRACT

Carbonates are abundant sedimentary minerals at the surface and sub-surface of the Earth and they have been proposed as tracers of liquid water in extraterrestrial environments. Their formation mechanism is since generally associated with aqueous alteration processes. Recently, carbonate minerals have been discovered on Mars' surface by different orbitals or rover missions. In particular, the phoenix mission has measured from 1% to 5% of calcium carbonate (calcite type) within the soil (Smith et al., 2009). These occurrences have been reported in area where the relative humidity is significantly high (Boynton et al., 2009). The small concentration of carbonates suggests an alternative process on mineral grain surfaces (as suggested by Shaheen et al., 2010) than carbonation in aqueous conditions. Such an observation could rather point toward a possible formation mechanism by dust–gas reaction under current Martian conditions. To understand the mechanism of carbonate formation under conditions relevant to current Martian atmosphere and surface, we designed an experimental setup consisting of an infrared microscope coupled to a cryogenic reaction cell (IR-CryoCell setup). Three different mineral precursors of carbonates (Ca and Mg hydroxides, and a hydrated Ca silicate formed from Ca_2SiO_4), low temperature (from -10 to $+30$ °C), and reduced CO_2 pressure (from 100 to 2000 mbar) were utilized to investigate the mechanism of gas–solid carbonation at mineral surfaces. These mineral materials are crucial precursors to form Ca and Mg carbonates in humid environments (0% < relative humidity < 100%) at dust–CO_2 or dust–water ice–CO_2 interfaces. Our results reveal a significant and fast carbonation process for Ca hydroxide and hydrated Ca silicate. Conversely, only a moderate carbonation is observed for the Mg hydroxide. These results suggest that gas–solid carbonation process or carbonate formation at the dust–water ice–CO_2 interfaces could be a currently active Mars' surface process. To the best of our knowledge, we report for the first time that calcium carbonate can be formed at a negative temperature (-10 °C) via gas–solid carbonation of Ca hydroxide. We note that the carbonation process at low temperature (< 0 °C) described in the present study could also have important implications on the dust–water ice–CO_2 interactions in cold terrestrial environments (e.g. Antarctic).

1. Introduction

The biotic and abiotic (i.e. chemical) formation of carbonates plays a crucial role in the global carbon cycle on Earth. In addition, carbonate minerals often sequester various trace elements (actinides and lanthanides), metalloids, and heavy metals, and thus control in part their global cycling (e.g. Paquette and Reeder, 1995; Stumm and Morgan, 1995; Sigg et al., 2000). In general, carbonate minerals can be formed in natural or artificial environments by three different mechanisms (e.g. Montes-Hernandez et al., 2010a): (1) aqueous nucleation-growth in homogeneous or heterogeneous systems (aqueous conditions), for example, the chemical or biogenic formation of carbonates in lakes, oceans, CO_2 storage sites, natural caves; (2) gas–solid carbonation of alkaline minerals (fine particles) in the presence of adsorbed water (water humidity conditions, 0 < water activity < 1), for example carbonate formation in water–unsaturated soils, in terrestrial or extraterrestrial aerosols (Shaheen et al., 2010). This water has an important role in the surface chemistry of minerals as was shown by Galhotra et al. (2009) and Baltrusaitis and Grassian (2005) with zeolites and iron oxide surfaces; (3) dry gas–solid carbonation of granular/porous materials (dry conditions, water activity ≈ 0), for example, the industrial mineralization, recovery or capture of CO_2 at high

* Corresponding author. Tel.: +33 607 9125 61.
** Corresponding author. Tel.: +33 683363044.
E-mail addresses: alexandre.garenne@ujf-grenoble.fr (A. Garenne), german.montes-hernandez@obs.ujf-grenoble.fr (G. Montes-Hernandez).

0032-0633/$ - see front matter © 2012 Elsevier Ltd. All rights reserved.
http://dx.doi.org/10.1016/j.pss.2012.11.005

temperatures in the presence of alkaline binary oxides (CaO, MgO) or metastable, nanoparticle alkaline silicates (Montes-Hernandez et al., 2012a, 2012b).

In the Planetary Sciences context, carbonates are generally considered as indicators of aqueous alteration processes (Bandfield et al., 2003; Milliken and Rivkin, 2009; Boynton et al., 2009; Ehlmann et al., 2008; Michalski and Niles, 2010). In the case of Mars, huge deposits of surface carbonates remained undetected for a long period, and their suspected absence was used to constrain the chemistry of a putative Martian ocean (Fairén et al., 2004). Evidences are now growing for the presence of carbonates at the surface of the red planet, which include observations of carbonate-rich outcrops (Ehlmann et al., 2008; Michalski and Niles, 2010) as well as carbonates within the Martian dust (Bandfield et al., 2003; Boynton et al., 2009). The aqueous alteration of mafic rocks in the presence of CO_2 is certainly an efficient mechanism for carbonate synthesis, an alternative pathway of carbonate synthesis exists, which does not require the presence of liquid water. This pathway involves reaction of a mineral substrate with CO_2 in the presence of chemisorbed water (few angstroms to few nm thick layers), and was recently tested and observed for terrestrial aerosols (Shaheen et al., 2010).

Here, we report on an experimental study of the kinetic of carbonation in liquid-water free environment. We designed novel, state of the art experimental setup (IR-CryoCell) to investigate the in situ gas–solid carbonation (i.e. resolved in time), for temperature and pressure conditions relevant to Mars. We studied carbonate synthesis starting from Ca and Mg hydroxides and an amorphous silicate (synthesized from Ca_2SiO_4), at low temperature (from -10 to $+30$ °C) and at low CO_2 pressure (from 100 to 2000 mbar). These starting materials are known precursors to form respective Ca and Mg carbonates in humid environments at dust–CO_2 or dust–water ice–CO_2 interfaces, at least under "terrestrial" conditions. They also can be expected to occur at the surface of Mars and some asteroids (Mg hydroxide has been described on Ceres). We report here laboratory experiments on gas–solid carbonation process at low temperature (<0 °C), which provides new insights on conditions for carbonate formation. We will show that gas–solid carbonation can occur below the water frost point (at terrestrial atmospheric pressure), with significant implications on the dust/water–ice/CO_2 interactions in cold environments.

2. Materials and methods

The experiments were performed using three different materials, Ca, Mg hydroxide and a Ca silicate hydrate. CO_2 is known to react with surface of CaO and MgO by adsorption (Ochs et al., 1998a, 1998b) and produce carbonates as well the importance of OH groups to water adsorption on surfaces (Yamamoto et al., 2008). These substrates were chosen to mimic natural conditions and to catalyze reaction as their surfaces are terminated by OH groups: (i) in order to form Ca–Mg carbonate by reaction with CO_2, a Ca and Mg source is needed; (ii) the presence of hydroxyl groups in the starting material was requested to permit auto-catalysis of the reaction (Montes-Hernandez et al., 2010a); (iii) the material had to be geologically relevant.

Brucite has not been detected on the Martian surface. However, various types of phyllosilicates have been now described over the planet that are interpreted as aqueous alteration products of mafic rocks (see the recent review by Ehlmann et al., 2011). Such aqueous alteration processes can be accompanied by the production of brucite (Evans, 2008). Identification of brucite by its spectral properties is difficult since no diagnostic band is present in the NIR, with the exception of the 2.7 μm feature ubiquitous to almost all –OH bearing phases. Brucite has been diagnosed on some asteroids from observations in the mid-IR (together with carbonate). It is the case of the largest main-belt object, Ceres. In addition, MgO has been proposed as a condensation product in some solar nebula models, which should readily transform to brucite in the presence of gaseous water or humidity (Gail and Sedlmayr, 1999).

Portlandite has not been reported on Mars either. On Earth, it is almost always found in association with calcium carbonates, and is very difficult to observe due to its high reactivity with CO_2. We chose to study portlandite because of its high catalytic reactivity which enabled to provide kinetic measurements under some hours. In addition, it is a structural analog to brucite and a number of X-$(OH)_2$ type hydroxide compounds (where X= Ni,Co,Fe,Mn,Cd). CaO has also been proposed as an intermediate compound by Shaheen et al. (2010) to explain the formation of calcium carbonate on Mars, which could readily transform to portlandite in the presence of gaseous H_2O or humidity.

Finally, we used an amorphous calcium silicate hydrate synthesized from larnite (Ca_2SiO_4). This material was chosen to represent an amorphous volcanic material. Volcanic activity has been widespread on Mars, and volcanoclastic deposits have been described (Ehlmann et al., 2011). We decided to use a pure calcium amorphous silicate (rather than a basaltic glass), in order to simplify the chemistry of the system. However, one might expect a more complex chemistry for Martian volcanic glasses. Our approach might appear too simplistic, but might provide grounds for understanding more complex chemistries.

2.1. Materials

2.1.1. Portlandite

Calcium hydroxide $Ca(OH)_2$ was provided by Sigma-Aldrich with 96% chemical purity (about 3% of $CaCO_3$) and 1% of other impurities. This material is characterized by platy nanoparticles (sheet forms) forming micrometric aggregates with high porosity and/or high specific surface area (15 m^2/g). Its infrared spectrum has revealed a small amount of adsorbed water at atmospheric conditions, around 0.01g H_2O/g $Ca(OH)_2$ determinated by TGA. The portlandite sample was used without any physicochemical treatment.

2.1.2. Brucite

Magnesium hydroxide $Mg(OH)_2$ was provided by Fisher Scientific (UK). This material is characterized by platy hexagonal microparticles. A small amount of adsorbed water at atmospheric conditions was detected by infrared spectroscopy. The brucite sample was crushed in a mortar before use.

2.1.3. Amorphous calcium silicate hydrate

This material was synthesized from synthetic larnite mineral (Ca_2SiO_4) by using a simple acidic treatment (2 M HCl solution) at room lab temperature during 15 minutes. Then, consecutive dilutions with demineralized water were carried out until pH equal to 3. Finally, the solid was separated from the solution by centrifugation (10 min at 12 000 rpm) and dried directly in the centrifugation flasks at 80 °C for 48 h. The larnite synthetic mineral was provided by Santos and it was synthesized as reported in Santos et al. (2009).

2.1.4. Carbon dioxide

Carbon dioxide CO_2 was provided by Linde Gas S.A. with 99.995% of chemical purity. This gas was directly injected in the cryogenic reaction cell without any treatment or purification.

2.2. Infrared microscope

An infrared microscope (BRUKER HYPERION 3000) coupled with a cryogenic cell (designed and built at IPAG) was used to obtain infrared spectra in transmission mode. The IR beam was focused trough a 15 × objective and the typical size of the spot on the sample was around $50 \times 50\ \mu m^2$. The spectral resolution was $4\ cm^{-1}$ and the spectra were recorded in transmission mode between $4000\ cm^{-1}$ and $700\ cm^{-1}$.

2.3. Cryogenic cell

An environmental cell was designed and built at IPAG in order to simulate low CO_2 pressure and low temperature (LP-LT) close to Martian atmospheric conditions. A heating resistance coupled to a liquid N_2 circuit (77 K) allows an efficient regulation of sample temperature from −180 °C to +100 °C. Additionally, a turbomolecular vacuum pump and a CO_2 cylinder were connected to reach a secondary vacuum and to inject a controlled CO_2 pressure into the reaction cell, respectively. Fig. 1 shows a schematic diagram of all main parts of the IR-CryoCell setup.

2.4. Gas–solid carbonation experiments

For these measurements, the reacting $Ca(OH)_2$ particles, stored at atmospheric conditions, were manually deposited and compressed as a thin film on a KBr window. Then the KBr window was carefully placed in the reaction cell to be assembled to the microscope. All carbonation experiments have been carried out in the presence of molecular water (adsorbed or crystallized as ice depending on the carbonation temperature) which catalyze the carbonation process. The carbonation temperatures used in this study were −10, 0, 10, 25 or 30 °C and the CO_2 pressures were typically 100, 1000 and 2000 mbar. This pressure is higher than Martian pressure to accelerate the reaction due to a daily timescale limitation by the experimental setup. We note that the CO_2 gas has been directly injected into the reaction cell in the presence or absence of atmospheric air. For the latter case, we started by fixing the water adsorbed onto the solid by cooling the cell at −60 °C before making a high vacuum pumping for 10 min in order to remove exclusively the air from the reaction cell. After injection of CO_2 10–15 infrared spectra have been collected as a function of time until an apparent spectroscopic equilibrium state is reached (3–6 h). Complementary carbonation experiments have been carried out by using Mg hydroxide (brucite: $Mg(OH)_2$) and the amorphous calcium silicate hydrate as solid reactants, but, for these cases the carbonation temperature has been fixed at 25 °C and 1 bar of CO_2 has been injected into the reaction cell without air removal (more reacting system).

Each carbonation experiment has been repeated two times in order to verify its reproducibility. All carbonation experiments and their physicochemical conditions are summarized in Table 1.

2.5. Calculation of integrated band intensities

The gas–solid carbonation of calcium hydroxide at low temperature (< 30 °C) in the presence of adsorbed water can be

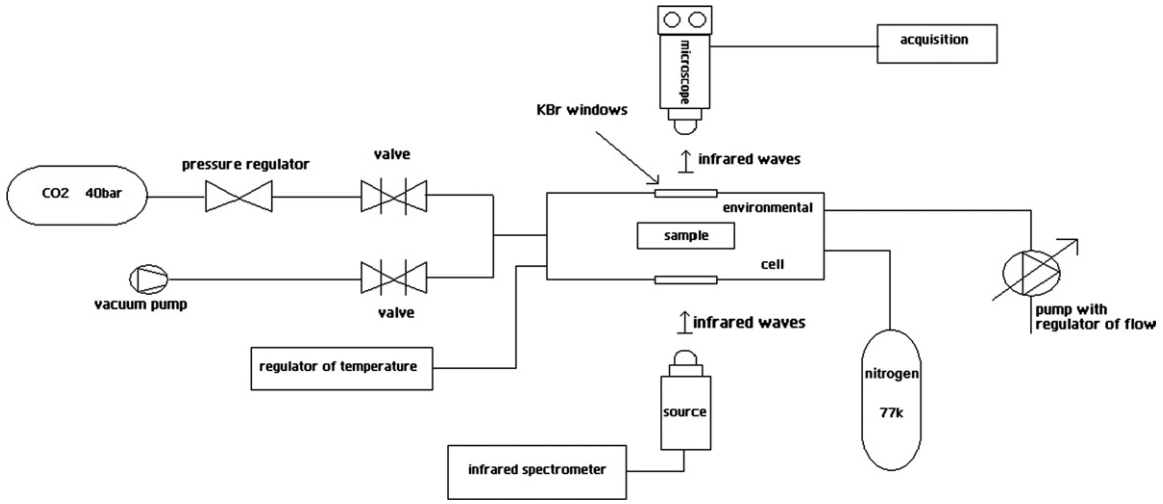

Fig. 1. Schematic representation of the IR-CryoCell experimental setup, showing the main parts such as temperature regulator, environmental cell, infrared microscope, valves, vacuum pump, CO_2 cylinder, liquid N_2 reservoir.

Table 1
Summary of the experiments with their experimental conditions and the corresponding kinetic parameters determined for gas–solid carbonation.

Exp.	Starting material	Gas pressure	Temperature (°C)	$A^{CO_3}_{max1}$ (a.u.)	$A^{CO_3}_{max2}$ (a.u.)	$t_{1/2_1}$ (min)	$t_{1/2_2}$ (min)	Ea (kJ/mol)
1	Portlandite	2 bar CO_2	−10	1.8	4.6	19.6	599.6	43
2	Portlandite	2 bar CO_2	0	6.4	0.8	8.9	8.9	
3	Portlandite	2 bar CO_2	10	5.3	11.4	61.8	61.8	
4	Portlandite	2 bar CO_2	25	29.3	54.8	2.5	126.6	
5	Portlandite,	1 bar CO_2+air,	−10	2.5	5	3.7	33 622	75
6	Portlandite	1 bar CO_2+air	0	5.4	10.2	6.3	28.5	
7	Portlandite	1 bar CO_2+air	10	15.8	3.1	3.5	180.1	
8	Portlandite	1 bar CO_2+air	30	26	21.2	3.5	5.8	
9	Portlandite	100 mbar, CO_2	25	19.8	10.9	0.8	419.1	
10	Brucite	1 bar CO_2+air	25	9.5	4.8	3	184.1	
11	Amorphous Ca silicate hydrate	1 bar CO_2+air	25	8.9	68	< 0.5	13.6	

Ea was calculated with Arrhenius equation. For experiments with 2 bar CO_2,we exclude the point of 10 °C due to his incoherence with Arrhenius equation.

expressed by a global reaction as follows:

$$Ca(OH)_2(s)+CO_2(g) \Rightarrow CaCO_3(s)+H_2O(v-l) \quad (1)$$

Generally, this global reaction is incomplete due to the formation of a protective carbonate layer around the reacting particle which restricts or stops the CO_2 transfer at the grain or aggregate scale (Montes-Hernandez et al., 2010a). In the present study, the integrated band intensities for hydroxyl (–OH), carbonate (CO_3^{2-}) and H_2O functional groups, concerning reaction (1) at an instant t have been estimated by using a Trapezoidal rule integration. A wavenumber interval and a characteristic continuum have been manually defined to determine the intensity of a given band depending on the initial reactant. For example, in the gas–solid carbonation experiments with $Ca(OH)_2$ particles, two continuums have been defined as linear segments over two different spectral ranges, one for the –OH at 3640 cm^{-1} and H_2O at 3450 cm^{-1} band intensities and the other for the H_2O at 1650 cm^{-1} and CO_3^{2-} at 1420 cm^{-1} band intensities (see Fig. 2).

2.6. Fitting of the kinetic experimental–calculated data for gas–solid carbonation

Several kinetic models (first-order, pseudo-first-order, second-order, pseudo-second-order, reversible one, irreversible one…) are generally used for fitting kinetic experimental data of sorption and adsorption systems (Ho and McKay, 1999; Ho, 2006). For our experiments, we have chosen pseudo-second-order model because it was successfully applied in previous studies (Montes and Geraud, 2004; Montes-Hernandez and Rihs, 2006; Montes-Hernandez et al., 2009, 2010a, 2010b, 2012a, 2012b) and can be adequately used to fit experimental data of carbonation process as demonstrated in Montes-Hernandez et al. (2009). This model reproduce a process consisting of a fast mass transfer followed by a second step of slower mass transfer until equilibrium is achieved. It can be written in its differential form as follows:

$$\frac{dA_{,t}^{CO_3}}{dt} = Kc\left(A_{,max}^{CO_3}-A_{,t}^{CO_3}\right)^2 \quad (2)$$

where $A^{CO_3}{}_{,t}$ is the integrated band intensity for the carbonate group at a given time, t [min], corresponding to carbonation extent; $A^{CO_3}{}_{,max}$ is the maximum extend of carbonation at equilibrium; Kc is the rate constant of $Ca(OH)_2$ carbonation.

The second step (until equilibrium) is interpreted by as a passivation effect due to the formation of a protective carbonate layer (Montes-Hernandez et al., 2012a). In this study, the increase of integrated band intensity with time for the carbonate group (CO_3^{2-}), i.e. during gas–solid carbonation process, has been fitted by using a kinetic double-pseudo-second-order model. This model assumes two kinetic regimes due to the presence of two types of reactive surface sites. The integrated form of the double kinetic model is given by the following hyperbolic equation:

$$A_{,t}^{CO_3} = \frac{\left(A_{,max1}^{CO_3}\right)t}{\left(t_{1/2_1}+t\right)} + \frac{\left(A_{,max2}^{CO_3}\right)t}{\left(t_{1/2_2}+t\right)} \quad (3)$$

where $A^{CO_3}{}_{,t}$ is the integrated band intensity for the carbonate group at a given time, t [min], corresponding to carbonation extent; $A_{,max1}^{CO_3}$ and $A_{,max2}^{CO_3}$ are the maximum extent of carbonation at apparent equilibrium for both kinetic carbonation regimes, respectively; $t_{1/2_1}$ and $t_{1/2_2}$ are the half-carbonation times for both kinetic carbonation regimes, respectively. In other terms, the half-carbonation times represent the times after which half of the maximum of kinetic carbonation regimes (expressed as maximum of integrated band intensities for carbonate group) is obtained. The fitting of kinetics data allow an estimation of these parameters and was performed by a non-linear regression by least-squares method. These simple parameters are used in this study to evaluate the kinetic effects of temperature, CO_2 pressure and nature of the solid on the gas–solid carbonation process.

The activation energy (Ea, Table 1) of the reaction was calculated assuming an Arrhenius behavior for the initial carbonation rate. We have used four points to calculate Ea for carbonation experiments of portlandite (at the temperature of −10 °C, 0 °C, 10 °C and 30 °C, for both experiments performed under 1 bar and 2 bar CO_2).

3. Results

3.1. Gas–solid carbonation of $Ca(OH)_2$ particles at low temperature (< 0 °C)

Very few experimental studies have characterized the carbonate formation or CO_2 mineralization at the mineral–ice water–CO_2 interfaces on Earth and planetary cold-environments (e.g. Antarctic and Mars surface). In our study, several gas–solid reactions carried out in the cryogenic cell coupled to the infrared microscope reveal that carbonate formation or CO_2 mineralization is possible at low temperature (−10 °C and 0 °C) using a simplified analogue $Ca(OH)_2$ (mineral)–water(adsorbed)–CO_2(gas) system (see Fig. 3(c)–(f)). The results displayed in Fig. 3 also reveal that the carbonation extent, monitored in situ by an increase of carbonate band intensity at 1420 cm^{-1}, is clearly inhibited by a decrease of temperature from 30 °C to −10 °C. The increase of integrated band intensity with time for the carbonate group at 1420 cm^{-1} has been successfully fitted by using the kinetic double-pseudo-second-order model. The experimental data and the calculated fits for six experiments are plotted in Fig. 4. This "a posteriori" modeling shows the good fits of all the experimental data by such type of kinetic model (correlation coefficient, R close to 1), and confirms the inhibition effect of temperature and the effect of relative humidity on the carbonation extent and kinetic parameters (see also Table 1).

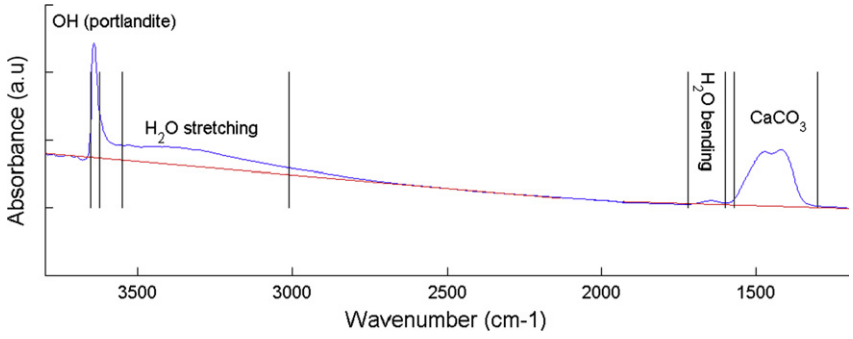

Fig. 2. Schematic representation for the calculation of the integrated band intensities of each functional group (–OH, H_2O, MCO_3), showing the continuum (in red) on an IR spectrum of portlandite. (For interpretation of the references to color in this figure caption, the reader is referred to the web version of this article.)

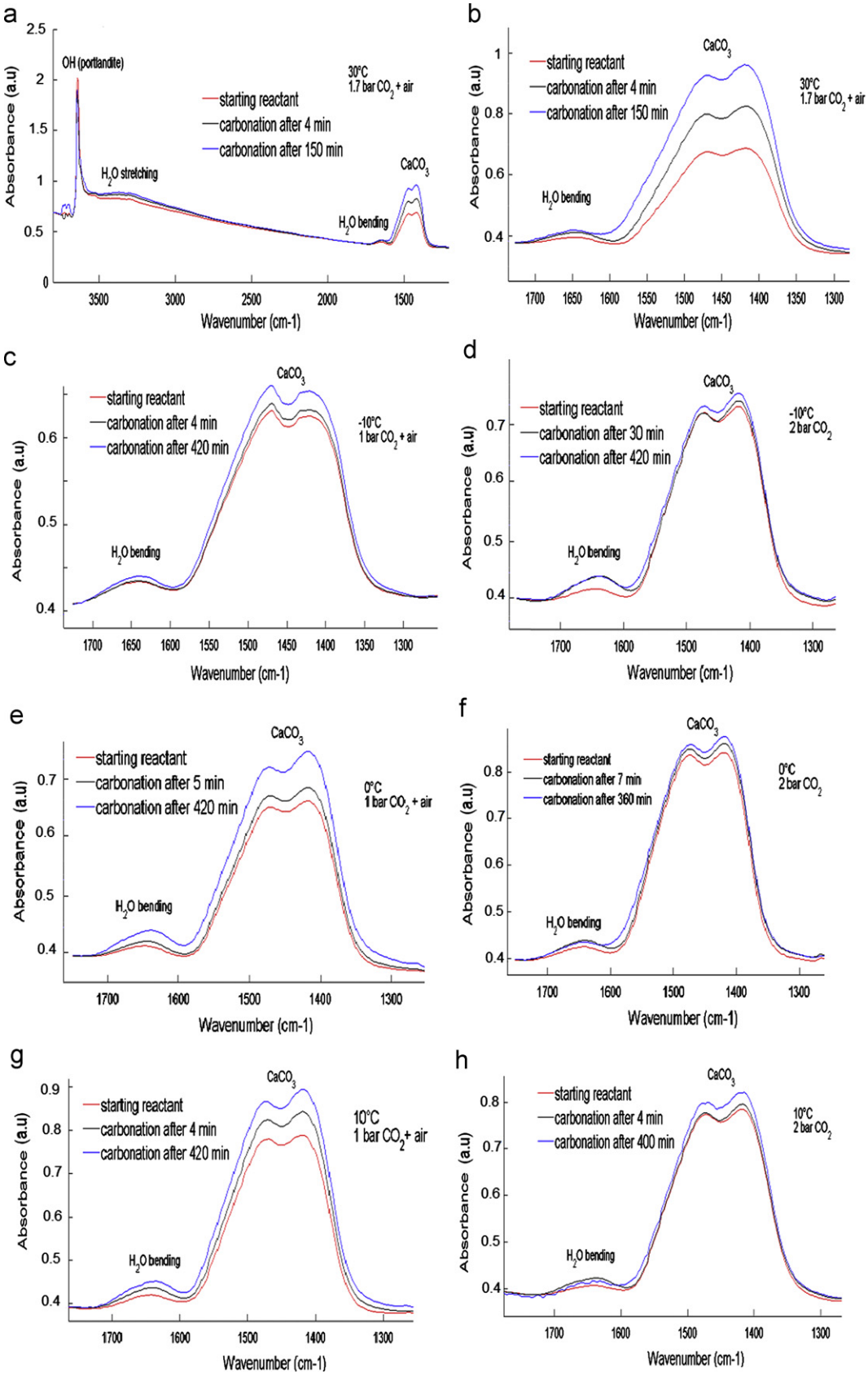

Fig. 3. Evolution with time of the IR spectrum of calcium carbonate during carbonation at different temperatures and CO_2 pressures. (a) Full IR spectrum of portlandite at 30 °C with 1.7 bar of CO_2 in the presence of air; (b) carbonate band at 30 °C under 1.7 bar of CO_2 with air; (c) at −10 °C under 1 bar of CO_2 with air; (d) at −10 °C under 2 bar of CO_2; (e) at 0 °C under 1 bar of CO_2 with air; (f) at 0 °C under 2 bar of CO_2; (g) at 10 °C under 1 bar of CO_2 with air and (h) at 10 °C under 2 bar of CO_2.

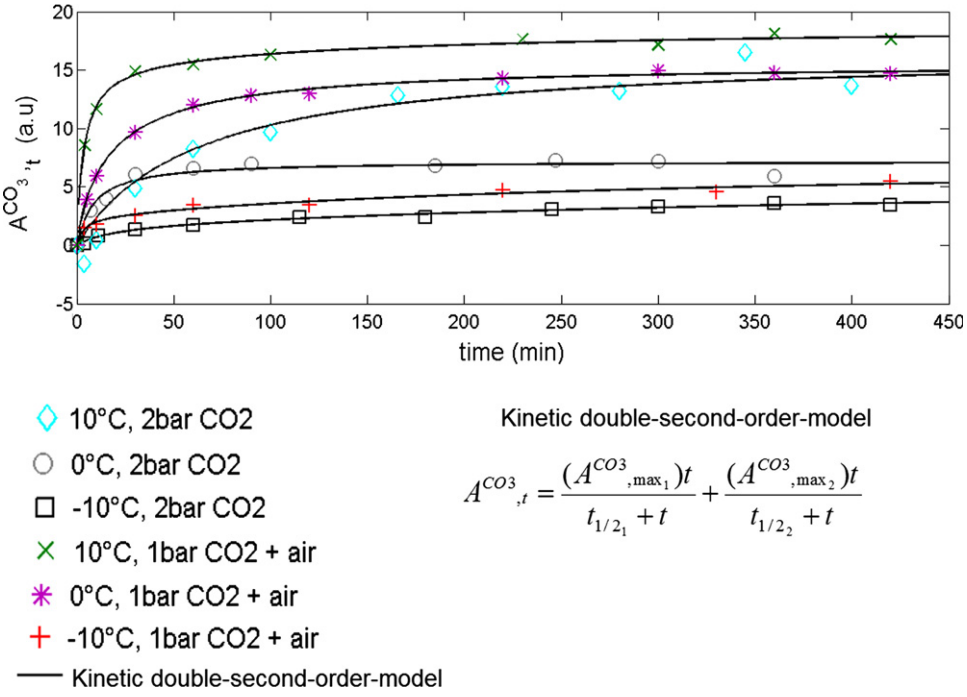

Fig. 4. Fits of the experimental kinetic data (carbonate band intensity) for gas–solid carbonation of Ca hydroxide (portlandite) in various experimental conditions by using a kinetic double-pseudo-second-order model and applying the non-linear least squares method.

One additional carbonation experiment with $Ca(OH)_2$ particles was carried out at low CO_2 pressure (100 mbar) and at moderate temperature (25 °C). For this case, the initial air contained into the cell was previously removed by pumping to secondary vacuum at low temperature (−60 °C) as explained in the materials and methods section. Here, a significant carbonation is observed after 4 min of $Ca(OH)_2$–CO_2 interaction followed by a very slow carbonation step until an apparent spectroscopic equilibrium is possibly reached (about 6 h) (see Fig. 5). These experimental data have been also successfully fitted by using the kinetic double-pseudo-second-order model. A last carbonation experiment was performed at a CO_2 pressure of 2 bar (at 25 °C) in order to compare with the low CO_2 pressure experiments. A significant carbonation was observed during all the experiment (see Fig. 6), which was fitted with the kinetic-pseudo-second order model.

3.2. Gas–solid carbonation of Mg hydroxide

The gas–solid carbonation depends also on the nature of the solid. For this reason one other powdered material, Mg hydroxide (synthetic brucite), was investigated specifically at higher reactive conditions (25 °C and 1 bar of CO_2, in presence of air). To form Mg carbonates, the most simple materials as starting reactant are binary oxides or hydroxides in the precursor material. Brucite particles are found to be only slightly carbonated at these T–P_{CO_2} conditions after 5.5 h of $Mg(OH)_2$-CO_2 interaction (see Fig. 7). These in situ infrared measurements clearly reveal that the Mg hydroxide (brucite) is more chemically stable than Ca hydroxide (portlandite) under a CO_2-rich atmosphere at a given relative humidity. In summary, the gas–solid carbonation of Ca and Mg hydroxides depends on the experimental conditions employed (i.e. T, P_{CO_2}, relative humidity) and on the intrinsic properties of solid (i.e. hydrophilicity, particle size, specific surface area, and chemical stability).

Finally, a kinetic regime and the maximum carbonation extent at an apparent equilibrium ($A^{CO_3}_{,max1}+A^{CO_3}_{,max2}$) is successfully determined by using a kinetic double-pseudo-second-order model (see Fig. 7(c)).

3.3. Gas–solid carbonation of an amorphous calcium silicate hydrate

A last material, an amorphous calcium silicate hydrate, has been investigated at higher reactive conditions (25 °C and 1 bar of CO_2, in presence of air) to test the gas–solid carbonation efficiency. The amorphous calcium silicate hydrate is significantly carbonated via gas–solid carbonation at the above mentioned T–P_{CO_2} conditions after 8 h of reaction (see Fig. 8), which suggests chemical stability has a significant impact on the efficiency of the carbonation.

Finally, a kinetic regime and the maximum carbonation extent at apparent equilibrium ($A^{CO_3}_{,max1}+A^{CO_3}_{,max2}$) is also successfully determined by using the kinetic double-pseudo-second-order model (see Fig. 8(c)).

4. The mechanism of carbonation

All the experiments with the Ca and Mg hydroxides show an increase of the band intensities of carbonates, at low temperature and low pressure. In this study we assume that part of the water initially adsorbed onto $Ca(OH)_2$ particles was partially crystallized by cooling when the temperature is negative (< 0 °C). The presence of an ice layer limits the access of CO_2 molecules to nanopores, and therefore limiting the CO_2 access to the local CO_3^{2-} production $\left(CO_2(g)+H_2O(adsorbed) \Rightarrow CO_3^{2-}+2H^+\right)$ required to form a carbonate layer around the $Ca(OH)_2$ particles (see also: Montes-Hernandez et al., 2010a). Strictly speaking, the relative humidity is not controlled in our experiments; however, two experiment protocols implying atmospheric vapor have been designed, first, direct injection of CO_2 gas into the reaction cell initially filled with air, i.e. at lab relative humidity (CO_2–air system) and second, the injection of CO_2 gas after removal of the air by secondary vacuum pumping at low temperature (−60 °C) (CO_2 system). The difference between these experiments could explain why the carbonation extent decreases when the initial air (contained into the reaction cell) is removed (see comparisons (c) and (d) or (e) and (f) in Fig. 3). We can assume a similar

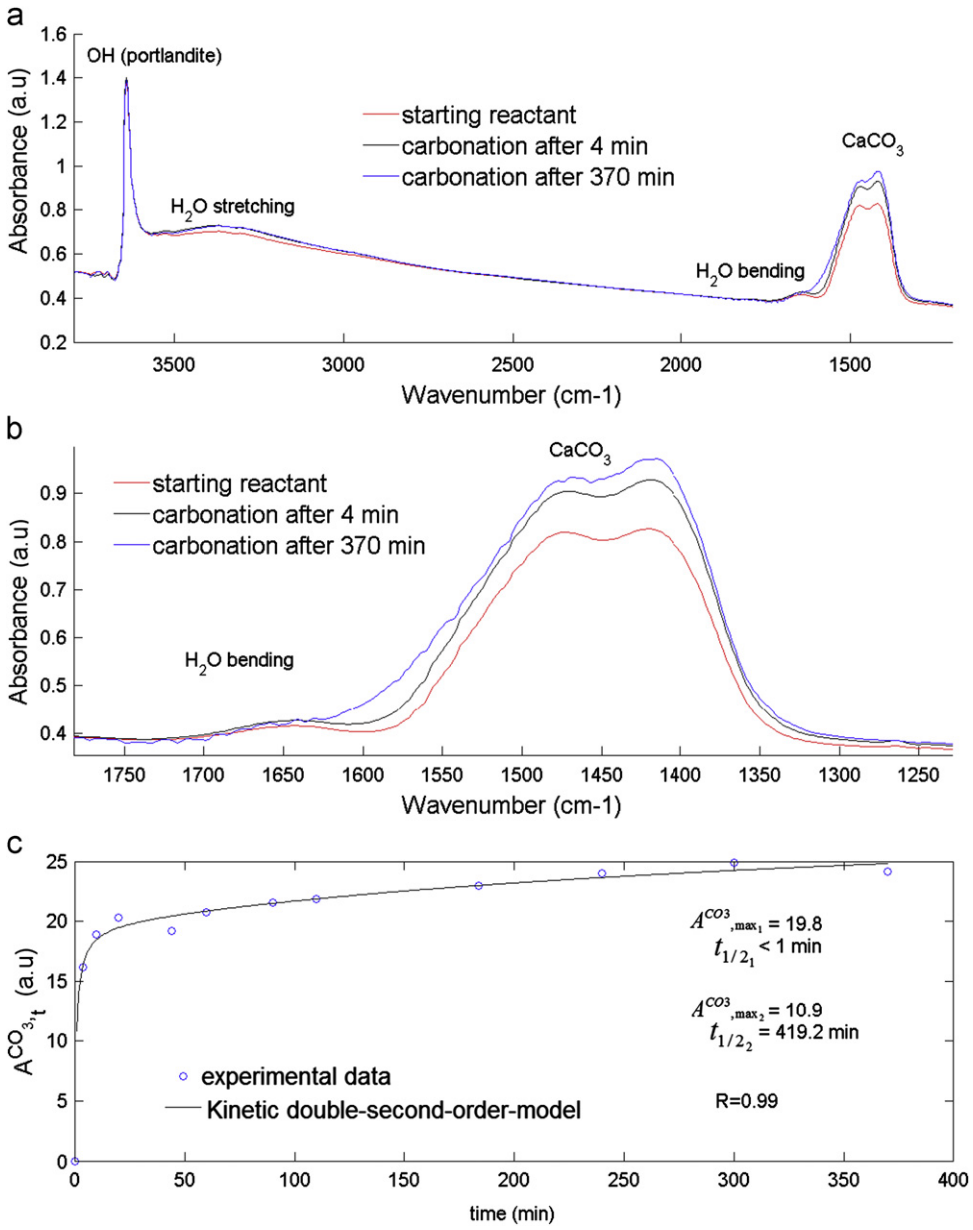

Fig. 5. Evolution with time of the IR spectrum of Ca hydroxide (portlandite) during carbonation at 25 °C under 100 mbar of CO_2: (a) Full spectrum. (b) Band of the carbonate group and (c) Fit of the experimental kinetic data (carbonate band intensity) for gas–solid carbonation by using a kinetic double-pseudo-second-order model and applying the non-linear least squares method.

relative humidity of the lab room for all experiments. This relative humidity has clearly an impact on the carbonation efficiency, the experiments without air (very low relative humidity) showing a lower amount of carbonation at low temperature.

The fit of the data by the kinetic model assumes two kinetic regimes, usually due to the presence of two types of reactive surface sites. In our carbonation experiments, the formation of a hydrated carbonate layer around the core of reacting $Ca(OH)_2$ particles produces a complex passivation step, possibly perturbed by three simultaneous physicochemical processes: (1) solid state transformation from hydrated calcium carbonate to calcite and/or from aragonite to calcite, (2) partial expelling of produced molecular water during the carbonation process (see Eqs. (1)) and (3) local acidification by an excess of molecular water in pores or onto surfaces ($H_2O(\text{produced}) + CO_2(g) \Rightarrow HCO_3^- + H^+$). In summary, the complex kinetic behavior related to gas–solid carbonation of $Ca(OH)_2$ particles is successfully described applying two kinetic regimes. A schematic representation of this carbonation process is illustrated in Fig. 9. The rate of carbonation depends on the access to the nanopores of the material by the CO_2. These pores have to be water-unsaturated to facilitate access of the CO_2 gas to react with the minerals. The pressure has a strong impact on the rate and yield of carbonation. In the case of the low pressure experiments, a two stage kinetic model was shown to fit the data. Experiments revealed a fast carbonation during a short time (stage 1) followed by a slower carbonation (stage 2). The magnitude of carbonate formation is high in stage 1 and lower in stage 2. In the case of the experiments performed at higher CO_2 pressure (2 bar) (Fig. 6(c)) a two stage reaction is also observed. However, unlike the low pressure experiments, the magnitude of carbonation achieved in stage 2 is quite significant.

For the low pressure experiments, we suspect that the intraparticle diffusion of CO_2, possibly limited by the low gas pressure in the system (100 mbar of CO_2), is the rate limiting step due to the carbonate layer which strongly reduce the diffusion of the gas. This

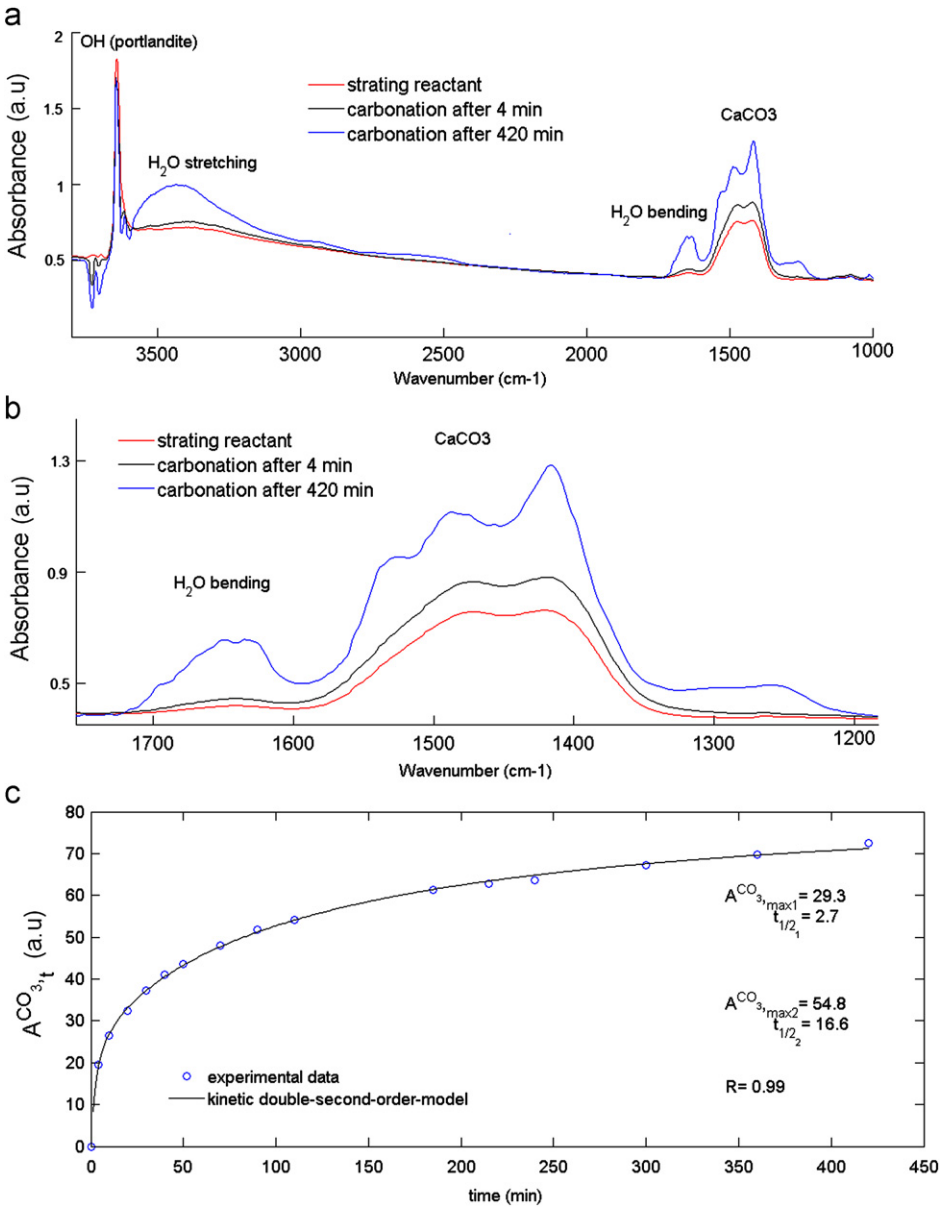

Fig. 6. Evolution with time of the IR spectrum of Ca hydroxide (portlandite) during carbonation at 25 °C under 2 bar of CO_2: (a) Full spectrum. (b) Band of the carbonate group and (c) Fit of the experimental kinetic data (carbonate band intensity) for gas–solid carbonation by using a kinetic double-pseudo-second-order model and applying the non-linear least squares method.

rate limiting step is no more observed at high CO_2 pressure (>20 bar). In this case, the $Ca(OH)_2$ particles are completely carbonated, leading to the formation of calcite nano-crystals (Montes-Hernandez et al., 2010b). We can assume a correlation between the pressure and the thickness of the layer that transforms to carbonate by gas–solid reaction. The effect of CO_2 pressure observed in explained by the presence of passivation step and the formation of carbonate layer through which CO_2 molecules have to diffuse. Therefore in the case of an uncarbonated material, the effect of CO_2 pressure on the initial reaction rate is expected to be moderate. Although the CO_2 pressure on Mars (about 10 mbar) is lower than CO_2 pressures used in our experiments (100 mbar), it is likely that our results can be extrapolated to Martian atmospheric CO_2 pressure.

Unfortunately, the gas–solid carbonation mechanism of amorphous calcium silicate hydrate is not elucidated due to its unknown atomic organization. However, we assume that the abundant molecular water adsorbed onto the solid plays a crucial role to start the gas–solid carbonation process at the investigated conditions. The in situ infrared measurements reveal two important insights: (1) The expelling of pre-existent molecular water in/on the solid towards the gas phase during the carbonation process. This is attested by a clear decrease of the stretching and bending band intensities of water (see Fig. 8(a) and (b)), (2) Similar to carbonation of Ca hydroxide, the formation of calcite and aragonite are mainly identified, the formation of hydrated calcium carbonate being only suspected (see also Montes-Hernandez et al., 2010a)

5. Discussion

Carbonates have been found on Mars in two kinds of geological settings: (i) outcrops of carbonates, identified in the Nili Fossae region (Ehlmann et al., 2008), in the central peak of Leighton crater (Michalski and Niles, 2010) and in the Columbia Hills of Gusev crater

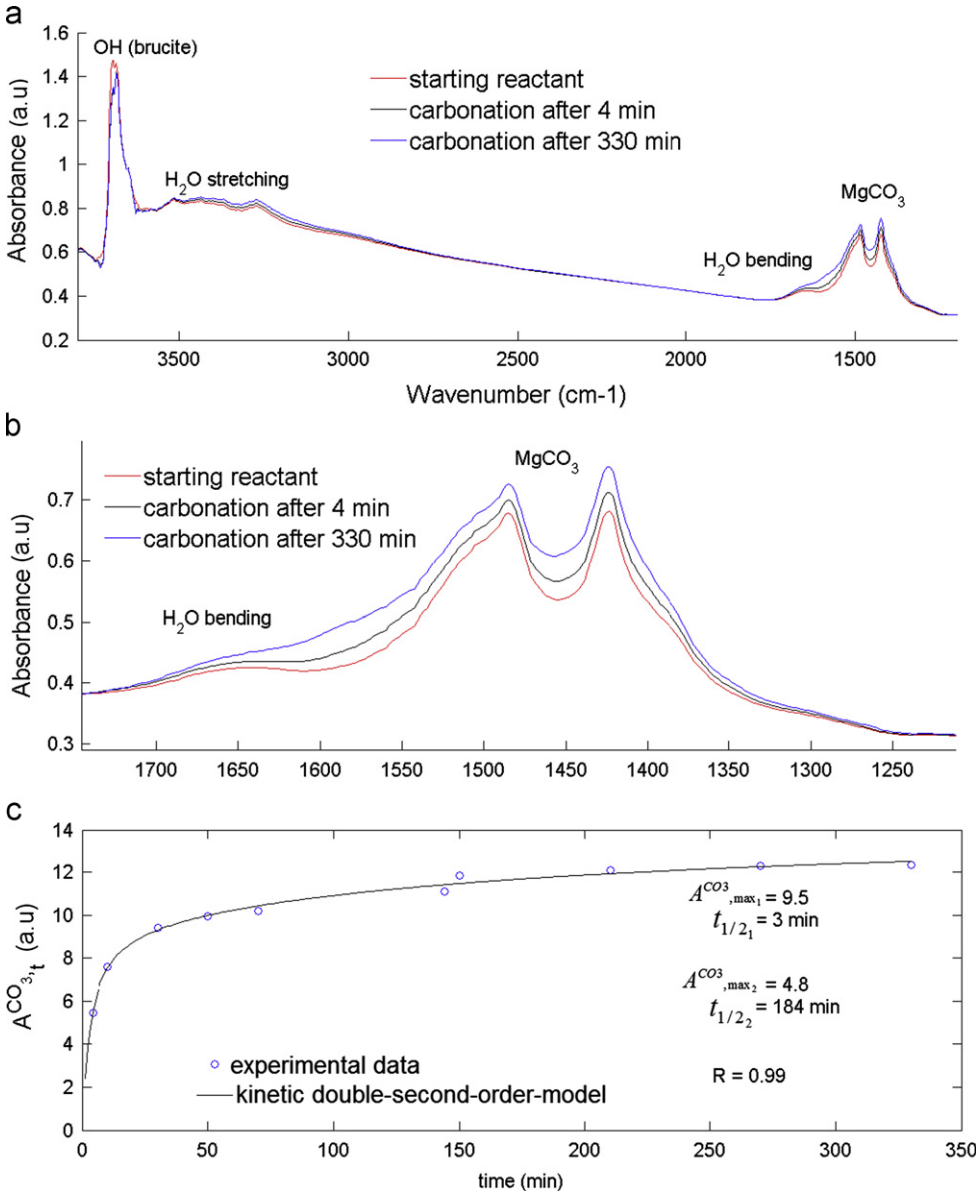

Fig. 7. Evolution with time of the IR spectrum of the Mg hydroxide (brucite) during carbonation at 25 °C under 1 bar of CO_2 with air: (a) Full spectrum. (b) Band of the carbonate group and (c) Fit of the experimental kinetic data (carbonate band intensity) for gas–solid carbonation by using a kinetic double-pseudo-second-order model and applying the non-linear least squares method.

(Morris et al., 2010); and (ii) carbonates-bearing dust, identified by the TES instrument (Bandfield et al., 2003) and the phoenix lander (Boynton et al., 2009). In the case of the outcrops from the Columbia Hills and Nili Fossae, carbonates are present as major components (16–34 wt% in the case of the Columbia Hills, about 80% in the case of Nili Fossae), and their derived chemistry is similar to that of carbonates found in Martian meteorites (Mittlefehldt, 1994), i.e. Fe–Mg carbonates. The association of these carbonate outcrops with phyllosilicates advocate for a possible hydrothermal origin of these carbonates, a phenomenon that has been reproduced in laboratory experiments (Golden et al., 2000) and that is observed in some terrestrial hydrothermal systems (Treiman et al., 2002; Brown et al., 2010). However, it is well known that terrestrial alteration of mafic rocks can produce brucite as a primary alteration product (Xiong and Snider Lord, 2008), which should readily transform into carbonate by interaction with the Martian atmosphere, according to our experiments. The observed carbonates outcrops could rather be former outcrops of brucite-rich sedimentary rocks that were subsequently altered to carbonates by interaction with the atmosphere.

In the case of carbonates observed in the Martian dust, both magnesite (Bandfield et al., 2003) and calcite (Boynton et al., 2009) have been reported, and their typical abundance is below 5%. Although aqueous formation has received widespread attention for this type of occurrence of carbonates on Mars, we propose gas–solid reaction as a possible formation mechanism. Calcite formation at the dust–CO_2 interfaces requires a source of calcium (e.g. Ca binary oxides or an amorphous metastable Ca silicate) possibly coming from volcanic activity (Shaheen et al., 2010), mechanical erosion or extra-Martian particulate matter (including meteorite impacts, interstellar dusts). A large diversity of phyllosilicates and hydrated phyllosilicates was found on the Martian surface (Mustard et al., 2008; Jänchen et al., 2006; Fairén et al., 2009; Murchie et al., 2009; Ehlmann et al., 2011). As we have shown, the presence of molecular water is also required

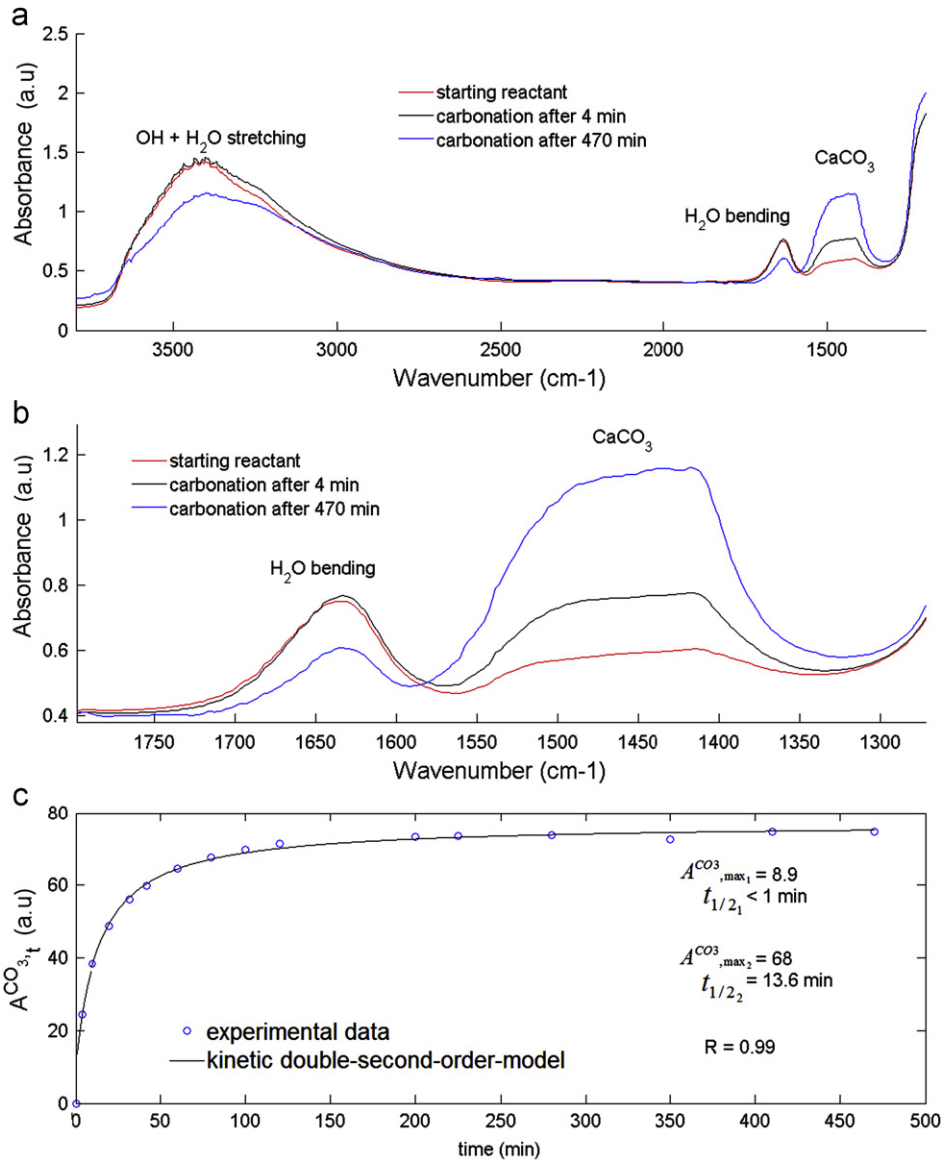

Fig. 8. Evolution with time of the IR spectrum of amorphous Ca silicate hydrate during carbonation at 25 °C under 1 bar of CO_2 with air: (a) Full spectrum. (b) Band of carbonate group and (c) Fit of the experimental kinetic data (carbonate band intensity) for gas–solid carbonation by using a kinetic double-pseudo-second-order model and applying the non-linear least squares method.

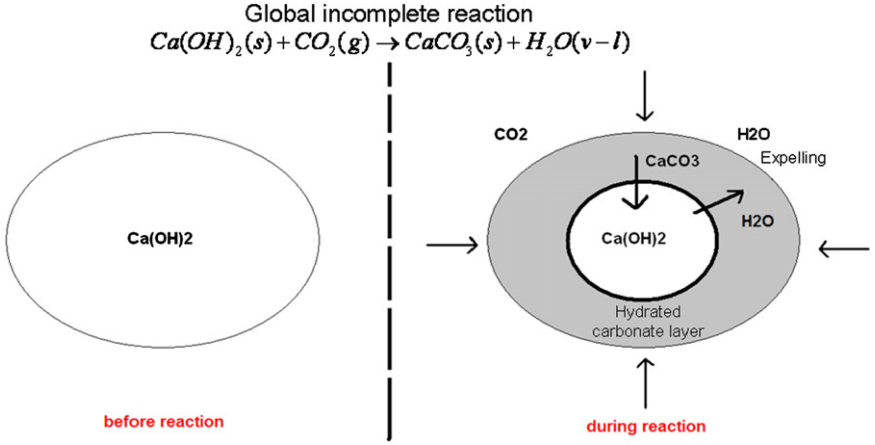

Fig. 9. Schematic representation of the gas–solid carbonation of Ca hydroxide, showing the growth of a hydrated calcium carbonate layer and the expelling of molecular water.

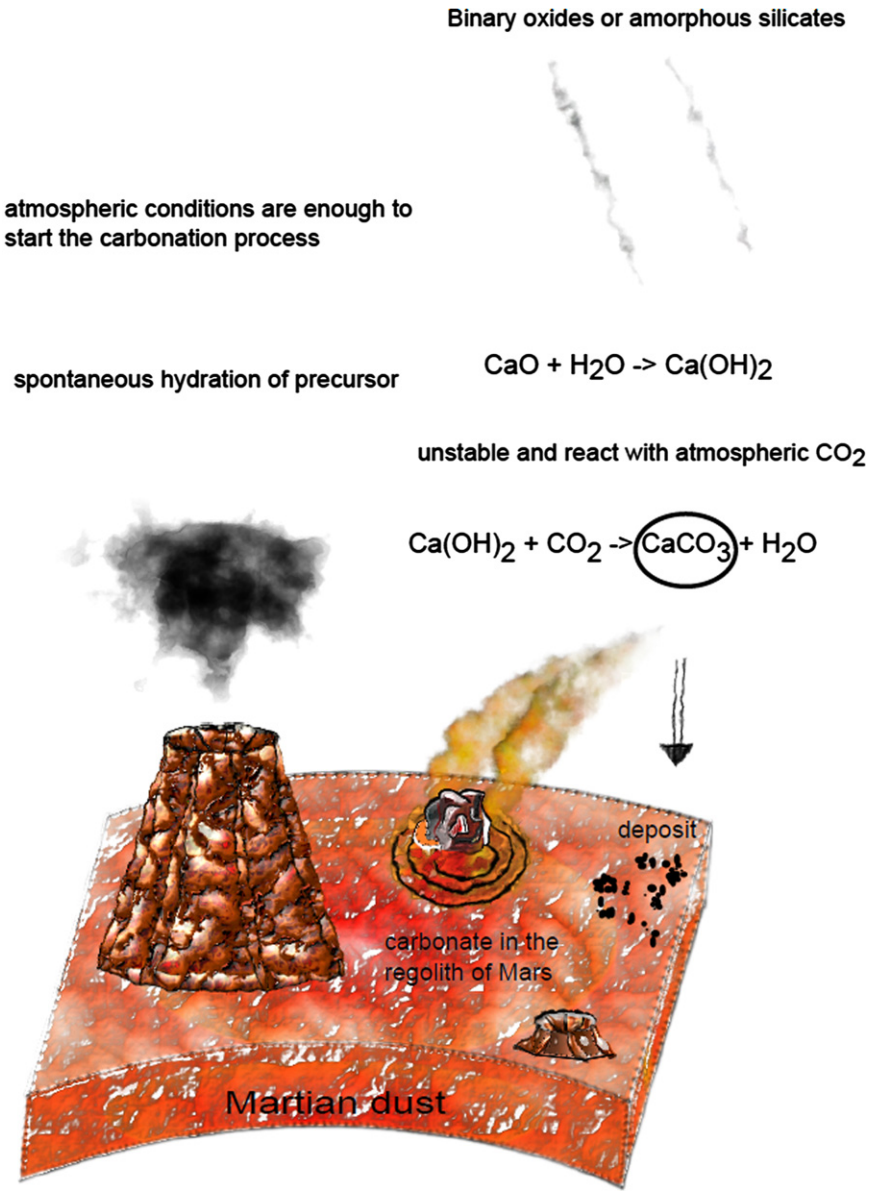

Fig. 10. A schematic representation of a possible current formation mechanism at dust–CO_2 interfaces of the calcium carbonate found at the Martian surface.

because hydration of the Ca precursor is assumed to be a crucial step prior to the carbonation process. Laboratory studies of Martian analogs suggest that adsorbed water should be present in significant amount within the Martian soil (Pommerol et al., 2009; Beck et al., 2010; Jänchen et al., 2006) and adsorbed water has been also detected by infrared spectroscopy (Poulet et al., 2009). In addition, the gamma rays and neutrons spectrometers on Mars Odyssey have shown evidence for the presence of water in the first meter of the Martian subsurface (Feldman et al., 2004). A simplified scenario for calcite formation at the dust–CO_2 interfaces and its natural deposition on the soil is schematically illustrated in Fig. 10. In this scenario we assume that the precursor, a calcium hydroxide with adsorbed water, is produced by atmospheric alteration of volcanic CaO particles in the atmosphere. Reactant minerals such as portlandite could be difficult to detect on Mars by reflectance spectroscopy due to the carbonate layer around the calcium hydroxide. In the case of hydromagnesite, the presence of brucite is required somewhere on Mars, which would be subsequently transformed to carbonates, eroded, and transported. As we stated earlier, brucite should form in association with phyllosilicates during the aqueous alteration of mafic rocks.

The efficiency of carbonates synthesis on Mars by gas–solid reaction will depend on the mineral substrate (as we showed, brucite, portlandite and larnite have distinct synthesis kinetics), the local temperature, the atmospheric humidity, and likely the atmospheric pressure (which can substantially vary with season as well as with topography). Even at temperatures below the frost point, carbonates synthesis can occur by gas–solid reaction, on a daily timescale (Table 1). On Mars, the water vapor pressure is low (P_{H_2O} about 10 Pa) and the frost point is depressed with regard to that on Earth. Given the present knowledge of the water vapor surface pressure, a typical value of 200 K is found for the frost point on the Martian surface (Schorghofer and Aharonson, 2005). Such temperature typically correspond to seasonal average around 60° in latitude.

The relative humidity on Mars fluctuates on a daily basis. At the Phoenix landing site (Smith et al., 2009) it is measured around 5% during Martian day time, close to saturation early night and

saturating at the end of the night. Carbonate synthesis will be accelerated by a high atmospheric humidity, which can occur during the warmer season. TES instrument on Mars Global Surveyor has water vapor evolution during two Martian years, and the maximum was found during midsummer in the northern hemisphere with 100 pr-μm (Smith, 2002, 2004). The maximum water vapor measured by Mars Express instruments (OMEGA and SPICAM) is found during midsummer, around 60 pr-μm content. This maximum is observed at latitude 75–80°N and longitudes 2109240°E (Fouchet et al., 2007; Fedorova et al., 2006; Melchiorri et al., 2007), an area is close to Phoenix landing site (latitude 68°N and longitude 233°E).

Current Global Circulation Models (GCM) of Mars can be used to determine the optimal locations and times for the gas–solid synthesis of carbonates. Simulations with Mars Climate Database (Forget et al., 1999, 2006) estimated high relative humidity (around 70%) and temperatures close to −20 °C during mid summer (L_s=120°) in the Phoenix landing site area (at 12 a.m.). These conditions are sufficient to initiate the carbonation reaction according to our experiments, and carbonates were observed in the Phoenix soil (Smith et al., 2009).

Mars is not the only extra-terrestrial body where carbonates have been detected, this is also the case of Ceres, the largest asteroid in the main belt. Its shape is close to hydrostatic equilibrium and its bulk density suggests the presence of ice in its interior (Thomas et al., 2005). The surface of Ceres shows a well-resolved 3-μm absorption band, which interpretation has been debated (Lebofsky et al., 1981; Vernazza et al., 2005; Rivkin et al., 2006; Rivkin et al., 2011; Beck et al., 2011). In a recent study, Milliken and Rivkin (2009) combined NIR and MIR observations of Ceres' surface and successfully modeled both spectral regions with a combination of brucite, carbonate and a Fe-rich phyllosilicate. Such a mineralogical assemblage was explained by aqueous alteration of mafic silicates in the presence of CO_2, by analogy with the processes inferred from the mineralogy of hydrated meteorites that can present a significant amount of carbonates (Zolensky et al., 2002). If brucite is rare in the mineralogy of hydrated chondrites, it is a common product of aqueous alteration of terrestrial rocks. The condition of brucite formation is specific in terms of T, pH and pO_2, and source rock. If the formation of carbonate by reaction of brucite with water is possible, gas–solid reaction cannot be excluded. This mechanism could occur at some depth in the asteroid body, where CO_2 pressure can build-up. However, because of the low temperature at the surface of Ceres, long timescales are expected for such a process. Further consideration would require an accurate knowledge of the kinetics of the gas–solid carbonation.

Finally, the carbonate synthesis mechanism that we described is certainly active on Earth, where carbonate minerals played an important role in the planet evolution. Many studies are available about carbonate reactivity and synthesis in liquid-water but information on its behavior at sub-zero temperatures (for example solubility in frozen water) are sparse. The results we obtained reveal that gas–solid carbonation can occur at sub-zero temperature, in the presence of gaseous CO_2 and H_2O. These conditions are present on Earth in arctic regions and in the upper atmosphere. This mechanism can thus occur on the availability of the adequate precursor.

The presence of oxygen isotope anomalies in carbonates from terrestrial aerosols (Shaheen et al., 2010) suggests a carbonation by exchange with ozone. Such a result suggests a possible formation of carbonate by chemical reaction in the upper atmosphere, from a CaO precursor. We can propose hydration of $CaO_{(s)}$ by $H_2O_{(g)}$, and successive reaction of $Ca(OH)_{2(s)}$ with $CO_{2(g)}$ as a formation mechanism of these carbonates.

Calcium carbonate and carbonate hydrates have been found in arctic ice (Dieckmann et al., 2008; Sala et al., 2008). The formation mechanism of these carbonates is a matter of active research, since it could provide a major CO_2 sequestration process. Hydrous carbonates (for instance ikaite) have been proposed to originate by precipitation during sea-ice formation, as suggested by thermodynamical calculations. Anhydrous carbonates can have an origin as primary aerosols, with a synthesis mechanism possibly similar to the one described in the previous paragraph. In addition, in situ gas–solid formation is possible, depending on the availability of an adequate precursor (as we showed here, an Ca or Mg hydroxides, or Ca-rich amorphous silicates).

6. Conclusion

In this study, we designed an original experimental method to form carbonates via gas–solid reaction in the presence of adsorbed water. We used an infrared microscope coupled to a cryogenic reaction cell (IR-CryoCell setup) to investigate this process with three different carbonate precursors (Ca hydroxide (portlandite), Mg hydroxide (brucite), and an amorphous calcium silicate hydrate). We demonstrated for the first time that calcium carbonate can be formed at low temperature (<0 °C) via gas–solid carbonation of Ca hydroxide. Both amorphous Ca silicate hydrate and Ca hydroxide were significantly carbonated at the investigated T–P_{CO_2} conditions. Conversely, only a very slight gas–solid carbonation of Mg hydroxide particles was detected by IR spectroscopy. We extracted the kinetic parameters of the reaction from our measured carbonation curves, following a kinetic double-pseudo-second-order model. From these results we can clearly state that the conditions for gas–solid carbonation exist on Mars, and that this process could be the source of the detected Ca and Mg carbonates found in the Martian dust and soil. These carbonates can be synthesized from a brucite precursor (a common hydrothermal product), from volcanic derived aerosols, as well as from extraterrestrial dust. This mechanism should be considered in future global modeling of the carbon cycle of the red planet, and might also be active in cold terrestrial deserts.

Acknowledgments

The authors are grateful to the French National Center for Scientific Research (CNRS), the French National Research Agency (ANR) and University Joseph Fourier (UJF) in Grenoble for providing the financial support.

References

Bandfield, J.L., Glotch, T.D., Christensen, P.R., 2003. Spectroscopic identification of carbonate minerals in the martian dust. Science 301, 1084–1087.
Beck, P., Pommerol, A., Schmitt, B., Brissaud, O., 2010. Kinetics of water adsorption on minerals and the breathing of the Martian regolith. Journal of Geophysical Research – Planets 115, E10011.
Beck, P., Quirico, E., Sevestre, D., Montes-Hernandez, G., Pommerol, A., Schmitt, B., 2011. Goethite as an alternative origin of the 3.1 mu m band on dark asteroids. Astronomy and Astrophysics 526, A85.
Baltrusaitis, J., Grassian, V.H., 2005. Surface reactions of carbon dioxide at the adsorbed water–iron oxide interface. The Journal of Physical Chemistry B 109, 12227–12230.
Boynton, W.V., Ming, D.W., Kounaves, S.P., Young, S.M.M., Arvidson, R.E., Hecht, M.H., Hoffman, J., Niles, P.B., Hamara, D.K., Quinn, R.C., Smith, P.H., Sutter, B., Catling, D.C., Morris, R.V., 2009. Evidence for calcium carbonate at the Mars Phoenix landing site. Science 325, 61–64.
Brown, A.J., Hook, S.J., Baldridge, A.M., Crowley, J.K., Bridges, N.T., Thomson, B.J., Marion, G.M., de Souza Filho, C.R., Bishop, J.L., 2010. Hydrothermal formation of Clay-Carbonate alteration assemblages in the Nil Fossae region of Mars. Earth and Planetary Science Letters 297, 174–182.
Dieckmann, G.S., Nehrke, G., Papadimitriou, S., Göttlicher, J., Steininger, R., Kennedy, H., Wolf-Gladrow, D., Thomas, D.N., 2008. Calcium carbonate as ikaite in Antartic sea ice. Geophysical Research Letters 35, L08501.

Ehlmann, B.L., Mustard, J.F., Murchie, S.L., Poulet, F., Bishop, J.L., Brown, A.J., Calvin, W.M., Clark, R.N., Des Marais, D.J., Milliken, R.E., Roach, L.H., Roush, T.L., Swayze, G.A., Wray, J.J., 2008. Orbital identification of carbonate-bearing rocks on Mars. Science 322, 1828–1832.

Ehlmann, B.L., Mustard, J.F., Murchie, S.L., Bibring, J.-P., Meunier, A., Fraeman, A.A., Langevin, Y., 2011. Subsurface water clay mineral formation during the early history of Mars. Nature 479, 53–60.

Evans, B.W., 2008. Control of the products of serpentinization by the Fe(2)Mg(1) exchange potential of olivine and orthopyroxene. Journal of Petrology 49, 1873–1887.

Fairén, A.G., Fernandez-Remolar, D., Dohm, J.M., Baker, V.R., Amils, R., 2004. Inhibition of carbonate synthesis in acidic oceans on early Mars. Nature 431, 423–426.

Fairén, A.G., Davila, A.F., Gago-Duport, L., Amils, R., McKay, C.P., 2009. Stability against freezing of aqueous solutions on early Mars. Nature 459, 401–404.

Fedorova, A., Korablev, O., Bertaux, J.-L., Rodin, A., Kiselev, A., Perrier, S., 2006. Mars water vapor abundance from SPICAM IR spectrometer: seasonal and geographic distributions. Journal of Geophysical Research 111, E09S08.

Feldman, W.C., Prettyman, T.H., Maurice, S., Plaut, J.J., Bish, D.L., Vaniman, D.T., Mellon, M.T., Metzger, A.E., Squyres, S.W., Karunatillake, S., Boynton, W.V., Elphic, R.C., Funsten, H.O., Lawrence, D.J., Tokar, R.L., 2004. Global distribution of near-surface hydrogen on Mars. Journal of Geophysical Research 109, E09006.

Forget, F., Hourdin, F., Fournier, R., Hourdin, C., Talagrand, O., Collins, M., Lewis, S.R., Read, P.L., Huot, J.-P., 1999. Improved general circulation models of the Martian atmosphere from the surface to above 80 km. Journal of Geophysical Research 1042, 24155–24176.

Forget, F., Millour, E., Lebonnois, S., Montabone, L., Dassas, K., Lewis, S.R., Read, P.L.,López-Valverde, M.A., González-Galindo, F., Montmessin, F., Lefèvre, F., Desjean, M.-C., & Huot, J.-P. 2006 (February). The new Mars climate database. In: F. Forget, M. A. Lopez-Valverde, M. C. Desjean, J. P. Huot, F. Lefevre, S. Lebonnois, S. R. Lewis, E. Millour, P. L. Read, & R. J. Wilson (Eds.), Mars Atmosphere Model ling and Observations, pp. 128.

Fouchet, T., Lellouch, E., Ignatiev, N.I., Forget, F., Titov, D.V., Tschimmel, M., Montmessin, F., Formisano, V., Guiranna, M., Maturilli, A., Encrenaz, T., 2007. Martian water vapor: Mars Express PFS/LW observations. Icarus 190, 32–49.

Gail, H.-P., Sedlmayr, E., 1999. Mineral formation in stellar winds. Astronomy and Astrophysics 347, 594–616.

Galhotra, P., Navea, J.G., Larsen, S.C., Grassian, V.H., 2009. Carbon dioxide ((CO_2)-O-16 and (CO_2)-O-18) adsorption in zeolite Y materials: effect of cation, adsorbed water and particle size. Energy and Environmental Science 2, 401–409.

Golden, D.C., Ming, D.W., Schwandt, C.S., Morris, R.V., Yang, S.V., Lofgren, G.E., 2000. An experimental study on kinetically-driven precipitation of calcium-magnesium-iron carbonates from solution: implications for the low-temperature formation of carbonates in martian meteorite Allan Hills 84001. Meteoritics & Planetary Science 35, 457–465.

Ho, Y.S., McKay, G., 1999. Pseudo-second order model for sorption processes. Process Biochemistry 34, 451–465.

Ho, Y.S., 2006. Review of second order models for adsorption systems. Journal of Hazardous Materials B136, 681–689.

Jänchen, J., Bish, D.L., Möhlmann, D.T.F., Stach, H., 2006. Investigation of the water sorption properties of Mars-relevant micro-and mesoporous minerals. Icarus 180, 353–358.

Lebofsky, L.A., Feierberg, M.A., Tokunaga, A.T., Larson, H.P., Johnson, J.R., 1981. The 1.7- to 4.2-micron spectrum of asteroid 1 Ceres: evidence for structural water in clay minerals. Icarus 48, 453–459.

Melchiorri, R., Encrenaz, T., Fouchet, T., Drossart, P., Lellouch, E., Gondet, B., Bibring, J.-P., Langevin, Y., Schmitt, B., Titov, D., Ignatiev, N., 2007. Water vapor mapping on Mars using OMEGA/Mars express. Planetary and Space Science 55, 333–342.

Michalski, J.R., Niles, P.B., 2010. Deep crustal carbonate rocks exposed by meteoritic impact on Mars. Nature Geoscience 3, 751–755.

Milliken, R.E., Rivkin, A.S., 2009. Brucite and carbonate assemblage from altered olivine-rich materials on Ceres. Nature Geoscience 2, 258–261.

Mittlefehldt, D.W., 1994. ALH84001, a cumulate othopyroxenite member of the Martian meteorite clan. Meteoritics 29, 214–221.

Montes-H, G., Geraud, Y., 2004. Sorption kinetic of water vapour of MX80 bentonite submitted to different physical–chemical and mechanical conditions. Colloids And Surfaces A – Physicochemical and Engineering Aspects 235, 17–23.

Montes-Hernandez, G., Rihs, S., 2006. A simplified method to estimate kinetic and thermodynamic parameters on the solid–liquid separation of pollutants. Journal of Colloid and Interface Science 299, 49–55.

Montes-Hernandez, G., Fernandez-Martinez, A., Renard, F., 2009. Novel method to estimate the linear growth rate of submicrometric calcite produced in a triphasic gas–liquid–solid system. Crystal Growth & Design 9, 4567–4573.

Montes-Hernandez, G., Pommerol, A., Renard, F., Beck, P., Quirico, E., Brissaud, O., 2010a. In situ kinetic measurements of gas-solid carbonation of $Ca(OH)_2$ by using infrared microscope coupled to a reaction cell. Chemical Engineering Journal 161, 250–256.

Montes-Hernandez, G., Daval, D., Chiriac, R., Renard, F., 2010b. Growth of nanosied calcite through gas–solid carbonation of nanosized portlandite under anisobaric conditions. Crystal Growth & Design 10, 4823–4830.

Montes-Hernandez, G., Chiriac, R., Toche, F., Renard, F., 2012a. Gas–solid carbonation of Ca(OH)2 and CaO particles under non-isothermal and isothermal conditions by using a thermogravimetric analyzer: implications for CO_2 capture. International Journal of Greenhouse Gas Control 11, 4172–4180.

Montes-Hernandez, G., Daval, D., Findling, N., Chiriac, R., Renard, F., 2012b. Linear growth rate of nanosized calcite synthesized via gas–solid carbonation of Ca(OH)2 particles in a static bed reactor. Chemical Engineering Journal 180, 237–244.

Morris, R.V., Ruff, S.W., Gellert, R., Ming, D.W., Arvidson, R.E., Clark, B.C., Golden, D.C., Siebach, K., Klingelhöfer, G., Schröder, C., Fleischer, I., Yen, A.S., Squyres, S.W., 2010. Identification of carbonate-rich outcrops on Mars by the Spirit Rover. Science 329, 421–424.

Murchie, S.L., Mustard, J.F., Ehlmann, B.L., Milliken, R.E., Bishop, J.L., McKeown, N.K., Noe Dobrea, E.Z., Seelos, F.P., Buczkowski, D.L., Wiseman, S.M., Arvidson, R.E., Wray, J.J., Swayze, G., Clark, R.N., Des Marais, D.J., McEwen, A.S., Bibring, J.-P., 2009. A synthesis of Martian aqueous mineralogy after 1 Mars year of observations from the Mars Reconnaissance Orbiter. Journal of Geophysical Research 114, E00D06.

Mustard, J.F., Murchie, S.L., Pelkey, S.M., Ehlmann, B.L., Milliken, R.E., Grant, J.A., Birbing, J.-P., Poulet, F., Bishop, J., Noe Dobrea, E., Seelos, F., Arvidson, R.E., Wiseman, S., Green, R., Humm, D., Malaret, E., McGovern, J.A., Seelos, K., Clancy, T., Clark, R., Des Marais, D., Izenberg, N., Knudson, A., Langevin, Y., Martin, T., McGuire, P., Robinson, M., Roush, T., Smith, M., Taylor, H., Titus, T., Wolff, M., 2008. Hydrated silicate minerals on Mars observed by the Mars Reconnaissance Orbiter CRISM instrument. Nature 454, 305–309.

Ochs, D., Braun, B., Maus-Friedrichs, W., Kempter, V., 1998a. CO_2 chemisorption at Ca and CaO surfaces: a study with MIES, UPS(HeI) and XPS. Surface Science 417, 406–414.

Ochs, D., Brause, M., Braun, B., Maus-Friedrichs, W., Kempter, V., 1998b. CO2 chemisorption at Mg and MgO surfaces: a study with MIES and UPS (He I). Surface Science 397, 101–107.

Paquette, J., Reeder, R.J., 1995. Relationship between surface structure, growth mechanism and trace element incorporation in calcite. Geochimica et Cosmochimica Acta 59, 735–749.

Pommerol, A., Schmitt, B., Beck, P., Brissaud, O., 2009. Water sorption on Martian regolith analogs: thermodynamics and near-infrared reflectance spectroscopy. Icarus 204, 114–136.

Poulet, F., Bibring, J.-P., Langevin, Y., Mustard, J.F., Mangold, N., Vincendon, M., Gondet, B., Pinet, P., Bardintzeff, J.-M., Platevoet, B., 2009. Quantitative compositional analysis of Martian mafic regions using the Mex/OMEGA reflectance data 1. Methodology, uncertainties and examples of application. Icarus 201, 69–83.

Rivkin, A.S., Volquardsen, E.L., Clark, B.E., 2006. The surface composition of Ceres: discovery of carbonates and iron-rich clays. Icarus 185, 563–567.

Rivkin, A.S., Li, J.Y., Milliken, R.E., Lim, L.F., Lovell, A.J., Schmidt, B.E., McFadden, L.A., Cohen, B.A., 2011. The surface composition of Ceres. Space Science Reviews 163, 95–116.

Sala, M., Delmonte, B., Frezzotti, M., Proposito, M., Scarchilli, C., Maggi, V., Artioli, G., Dapiaggi, M., Marino, F., Ricci, P.C., De Giudici, G., 2008. Evidence of calcium carbonates in coastal (Talos Dome and Ross Sea area) East Antarctica snow and firn: Environmental and climatic implications. Earth and Planetary Science Letters 271, 43–52.

Santos, A., Ajbary, M., Morales-Flórez, V., Kherbeche, A., Pi˜nero, M., Esquivias, L., 2009. Larnite powders and larnite/silica aerogel composites as effective agents for CO_2 sequestration by carbonation. Journal of Hazardous Materials 168, 1397–1403.

Schorghofer, N., Aharonson, O., 2005. Stability and exchange of subsurface ice on Mars. Journal of Geophysical Research 110, E05003.

Shaheen, R., Abramian, A., Horn, J., Dominguez, G., Sullivan, R., Thiemens, M.H., 2010. Detection of oxygen isotopic anomaly in terrestrial atmospheric carbonates and its implications to Mars. Proceedings of the National Academy of Sciences of the United States of America 107, 20213–20218.

Sigg, L., Xue, H., Kistker, D., Schönenberger, R., 2000. Size fractionation (dissolved, colloidal and particulate) of trace metals in the Thur River, Switzerland. Aquatic Geochemistry 6, 413–434.

Smith, M.D., 2002. The annual cycle of water vapor on Mars as observed by the thermal emission spectrometer. Journal of Geophysical Research 107, E11,5115.

Smith, M.D., 2004. Interannual variability in TES atmospheric observations of Mars during 1999–2003. Icarus 167, 148–165.

Smith, M.D., Wolff, M.J., Clancy, R.T., Murchie, S.L., 2009. Compact reconnaissance imaging spectrometer observations of water vapor and carbon monoxide. Journal of Geophysical Research 114, E00D03.

Smith, P.H., Tamppari, L.K., Arvidson, R.E., Bass, D., Blaney, D., Boynton, W.V., Carswell, A., Catling, D.C., Clark, B.C., Duck, T., DeJong, E., Fisher, D., Goetz, W., Gunnlaugsson, H.P., Hecht, M.H., Hipkin, V., Hoffman, J., Hviid, S.F., Keller, H.U., Kounaves, S.P., Lange, C.F., Lemmon, M.T., Madsen, M.B., Markiewicz, W.J., Marshall, J., McKay, C.P., Mellon, M.T., Ming, D.W., Morris, R.V., Pike, W.T., Renno, N., Staufer, U., Stoker, C., Taylor, P., Whiteway, J.A., Zent, A.P., 2009. H_2O at the phoenix landing site. Science 325, 58–61.

Stumm, W., Morgan, J.J., 1995. Aquatic Chemistry – Chemical Equilibria and Rates in Natural Waters, Third Edition John Wiley & Sons Inc., New York.

Thomas, P.C., Parker, JWm, McFadden, L.A., Russel, C.T., Stern, S.A., Sykes, M.V., Young, E.F., 2005. Differentiation of the asteroid Ceres as revealed by its shape. Nature 437, 224–226.

Treiman, A.H., Amundsen, H.E.F., Blake, D.F., Bunch, T., 2002. Hydrothermal origin for carbonate globules in Martian meteorite ALH84001: a terrestrial analogue from Spitsbergen (Norway). Earth and Planetary Science Letters 204, 323–332.

Vernazza, P., Mothé-Diniz, T., Barucci, M.A., Birlan, M., Carvano, J.M., Strazzulla, G., Fulchignoni, M., Migliorini, A., 2005. Analysis of near-IR spectra of 1 Ceres and 4 Vesta, targets of the Dawn mission. Astronomy and Astrophysics 436, 1113–1121.

Xiong, Y., Snider Lord, A., 2008. Experimental investigations of the reaction path in the $MgO–CO_2–H_2O$ system in solutions with various ionic strengths, and their applications to nuclear waste isolation. Applied Geochemistry 23, 1634–1659.
Yamamoto, S., Bluhm, H., Andersson, K., Ketteler, G., Ogasawara, H., Salmeron, M., Nilsson, A., 2008. In situ X-ray photoelectron spectroscopy studies of water on metals and oxides at ambient conditions. Journal of Physics: Condensed Matter 20, 84025.
Zolensky, M.E., Nakamura, K., Gounelle, M., Mikouchi, T., Kasama, T., Tachikawa, O., Tonui, E., 2002. Mineralogy of Tagish Lake: an ungrouped type 2 carbononaceous chondrite. Meteoritics & Planetary Science 37, 737–761.